Reliable aeroacoustic simulation on unstructured grids with OpenFOAM

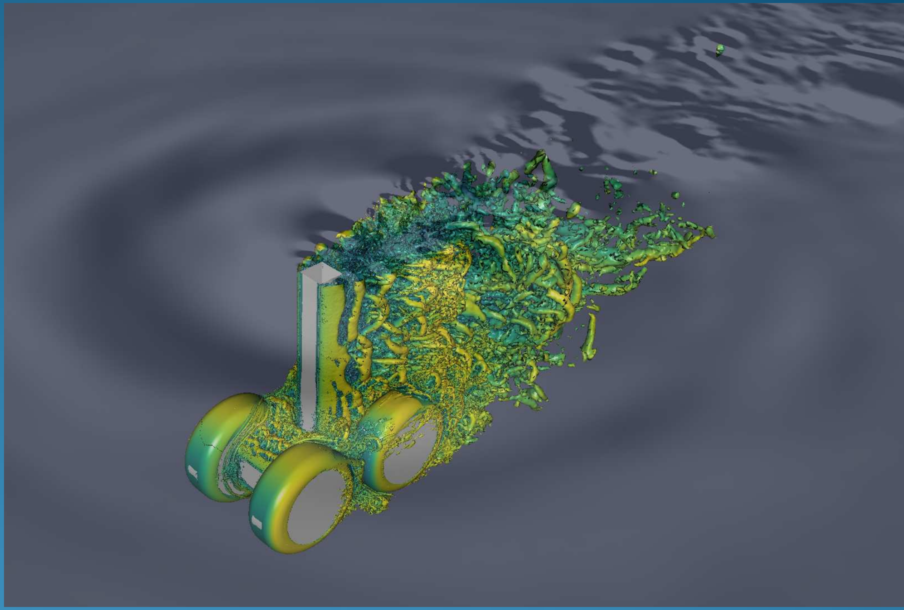

M. Fuchs[1], C. Mockett[1], F. Kramer[1], T. Knacke[1], D. Fischer[2] & F. Thiele[1]

charles.mockett@cfd-berlin.com

1) CFD Software E+F GmbH
CFD Software Entwicklungs- und Forschungsgesellschaft mbH
Berlin, Germany

2) TU berlin cfd caa
Berlin, Germany

Introduction

Enhanced aeroacoustics features in OpenFOAM

- Improved aeroacoustics solver for low Mach number applications
- Efficient input / output library for FW-H analysis
- Improved hybrid RANS-LES turbulence modelling

Validation for Rudimentary Landing Gear

- Test case setup
- Solver comparison
- Mesh comparison

Conclusions and next steps

Introduction

Enhanced aeroacoustics features in OpenFOAM

- Improved aeroacoustics solver for low Mach number applications
- Efficient input / output library for FW-H analysis
- Improved hybrid RANS-LES turbulence modelling

Validation for Rudimentary Landing Gear

- Test case setup
- Solver comparison
- Mesh comparison

Conclusions and next steps

Introduction

- Goal: Reliable, source-resolving, direct aeroacoustic prediction for industrial geometries at low Mach numbers
- Requirements on simulation process chain:
  - Compressible solver with low spurious numerical noise
  - High-fidelity scale-resolving turbulence model
  - Non-reflecting boundary conditions
  - Sponge layer for small domains
  - Method for far-field wave propagation (e.g. Ffowcs Williams & Hawkings)
  - Efficient output of unsteady data
  - **Unstructured grids for complex geometries**
- All items have been implemented and validated, but so far only on structured meshes
- First results for the Rudimentary Landing Gear (RLG) test case on an unstructured grid will be presented

Blind partner results for Rudimentary Landing Gear (RLG) at BANC-II workshop

Spalart & Wetzel, 2015

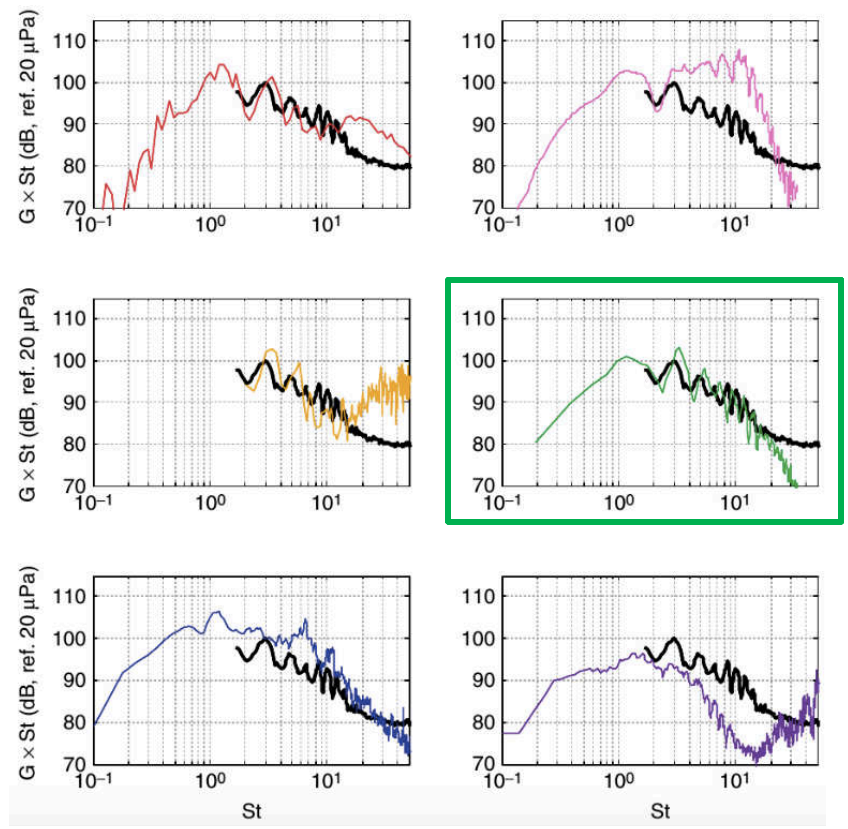

Introduction

Enhanced aeroacoustics features in OpenFOAM

- Improved aeroacoustics solver for low Mach number applications
- Efficient input / output library for FW-H analysis
- Improved hybrid RANS-LES turbulence modelling

Validation for Rudimentary Landing Gear

- Test case setup
- Solver comparison
- Mesh comparison

Conclusions and next steps

Improved aeroacoustics solver for low Mach number applications

- For low Mach number flows, pressure-based solvers are often an efficient choice (relative to e.g. density-based solvers)
- Unfortunately, numerical implementation details can have a large influence on the prediction of aeroacoustics especially at low Mach numbers:
  - Physical noise sources are very quiet for low Mach number applications, thus greater sensitivity to additional spurious noise from numerics
- We worked extensively on the Rhie & Chow interpolation implementation in OpenFOAM, which is the core mechanism to couple velocity and pressure fields for pressure-based solvers:

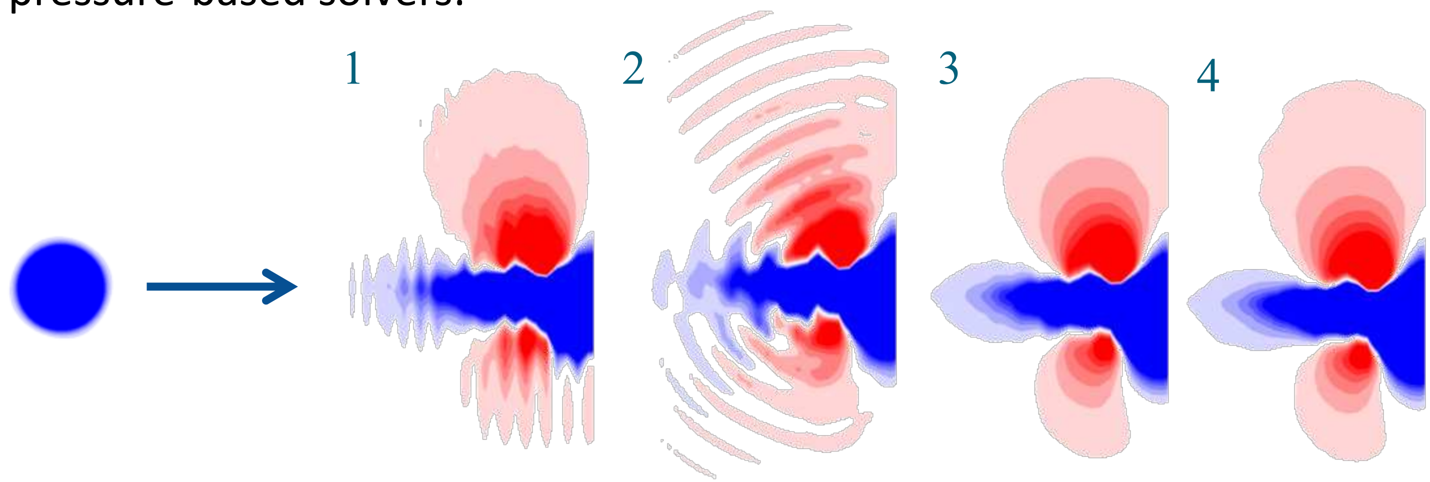

Aeroacoustics post-processing

- Our aim:
  - Development of efficient, solver-independent process chain for farfield noise prediction
- Our process chain consists of two separate tools, which use a common file format
- *effIO*: efficient library for input / output:
  - External solver-independent dynamic library which is linked to OpenFOAM solver at run-time
  - Reads surface description from STL / ASCII input
  - Writes unsteady FW-H data from surfaces in predefined format (HDF5)
- In-house FW-H tool for farfield integration:
  - Uses *effIO* library to read unsteady FW-H data
  - Performs sound integration to farfield

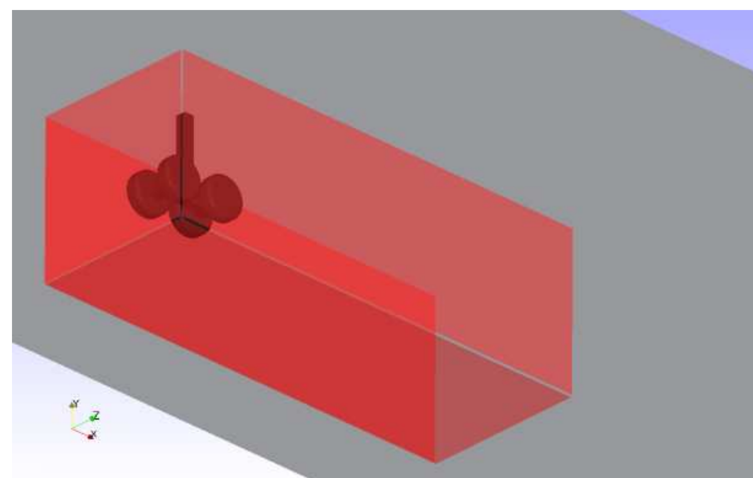

defined permeable FW-H surfaces in STL format

effIO = efficient library for input/output

- Key features of *effIO* library:
  - Solver-independent library for consistent post-processing between different CFD solvers
  - Simple integration with minimal impact on solver
  - Output specification outside of solver in a common configuration file (cross-solver)
  - Parallel IO support
  - Writes one single file for each FW-H surface containing all variables
  - Temporal buffering for unsteady data: multiple time steps in one file → reduces IO overhead and number of output files
  - On-the-fly data manipulation:
    - Computation of temporal mean /max, temporal exponential smoothing, etc.
  - Allows data reduction
  - A clear on-disk data layout

Enhanced hybrid RANS-LES modelling

- Delayed DES (DDES) with accelerated "RANS-to-LES transition"
- Details of formulation published:

  C. Mockett, M. Fuchs, A. Garbaruk, M. Shur, P. Spalart, M. Strelets, F. Thiele, A. Travin: Two non-zonal approaches to accelerate RANS to LES transition of free shear layers in DES. In: *Progress in Hybrid RANS-LES Modelling,* NNFM Vol 130, Springer (2015)
- Two key ingredients:
  - An adaptive definition of the grid filter, denoted $\tilde{\Delta}_\omega$
  - Alternative form of SGS model in LES mode region, i.e. the σ-model of Nicoud et al.

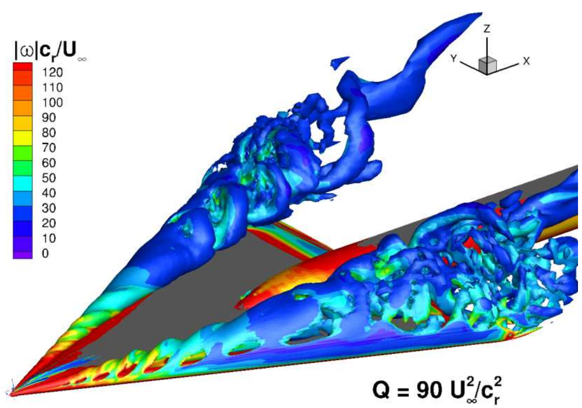

SA-DDES + Δ_{max}

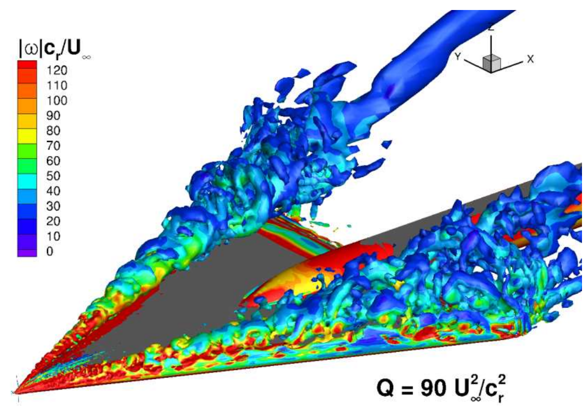

SA-σ-DDES + $\tilde{\Delta}_\omega$

Enhanced hybrid RANS-LES modelling

- Delayed DES (DDES) with accelerated "RANS-to-LES transition"
- Details of formulation published:

  C. Mockett, M. Fuchs, A. Garbaruk, M. Shur, P. Spalart, M. Strelets, F. Thiele, A. Travin: Two non-zonal approaches to accelerate RANS to LES transition of free shear layers in DES. In: *Progress in Hybrid RANS-LES Modelling,* NNFM Vol 130, Springer (2015)

- Two key ingredients:
  - An adaptive definition of the grid filter, denoted $\tilde{\Delta}_{\omega}$
  - Alternative form of SGS model in LES mode region, i.e. the σ-model of Nicoud et al.

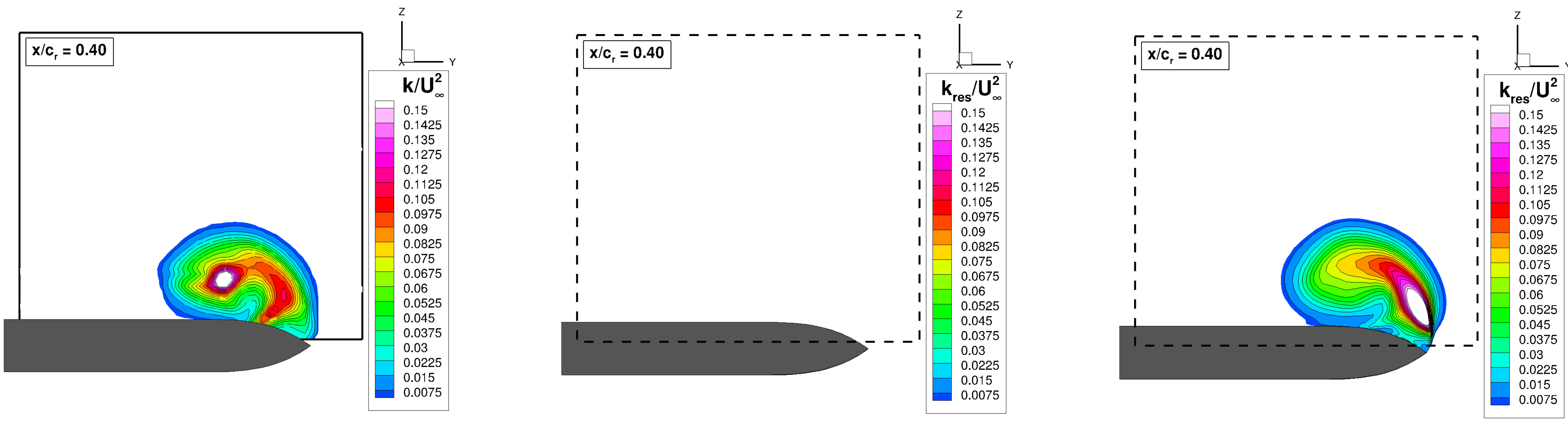

Exp (HWA) **SA-DDES + Δ_{max}** **SA-σ-DDES + $\tilde{\Delta}_{\omega}$**

Introduction

Enhanced aeroacoustics features in OpenFOAM

- Improved aeroacoustics solver for low Mach number applications
- Efficient input / output library for FW-H analysis
- Improved hybrid RANS-LES turbulence modelling

Validation for Rudimentary Landing Gear

- Test case setup
- Solver comparison
- Mesh comparison

Conclusions and next steps

Rudimentary landing gear (RLG)

- Test case was part of 2012 AIAA BANC-II aeroacoustics benchmarking workshop
- Aerodynamic and acoustic measurement data available
- Test case properties:
  - Generic 4-wheel landing gear configuration mounted on ceiling
  - $Re_D = 1.0 \times 10^6, M = 0.12$
- Existing results for in-house solver on structured grid from *Wang et al. "Detached-Eddy Simulation of Landing-Gear Noise", 19th AIAA/CEAS Aeroacoustics Conference, (AIAA 2013-2069)*

Aerodynamic measurements at National Aerospace Laboratories, Bangalore / India

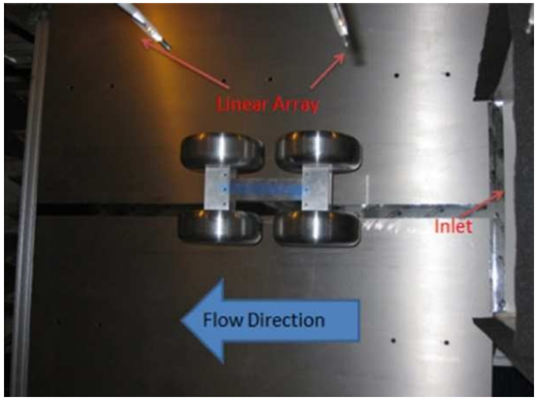

Aeroacoustics measurements at University of Florida / USA

Test case setup

- Flow solver (OF-v3.0+):
  - Fully compressible pressure-based branch with multiple sub-iterations: standard OF solver is *rhoPimpleFoam*
- Turbulence model:
  - Grey-area enhanced SA-σ-DDES + $\widetilde{\Delta}_{\omega}$
- Discretisation schemes & time step size:
  - Hybrid convection scheme of Travin et al. For advection term: blending between 2^{nd} order CDS / upwind-biased scheme
  - 2^{nd} order implicit Euler scheme for time
  - $\Delta t = 0.005 \times D/U_{\infty}$
- Convergence criteria:
  - 1 order of magnitude reduction for p
  - 3 orders of magnitude reduction for U, h, υ_t
- 32.5-70 CTU computed for acoustic statistics

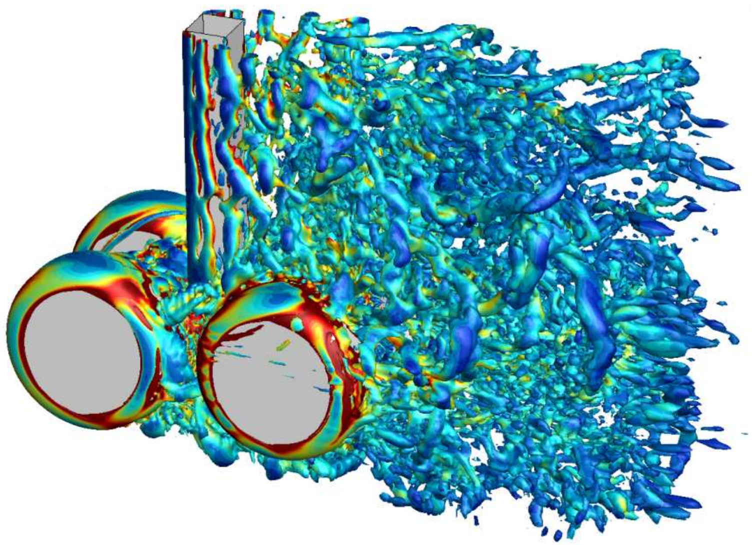

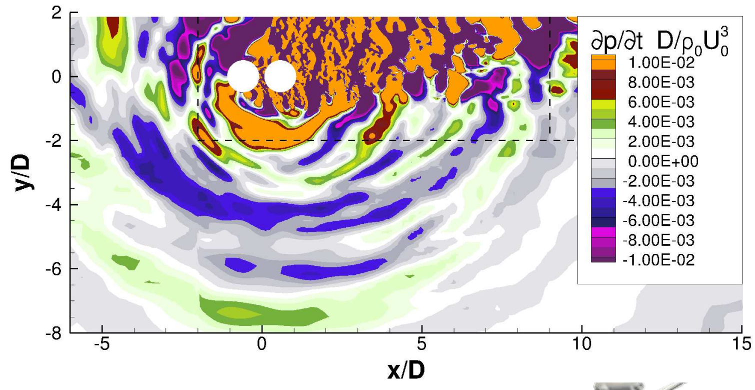

Structured and unstructured grids

Structured grid

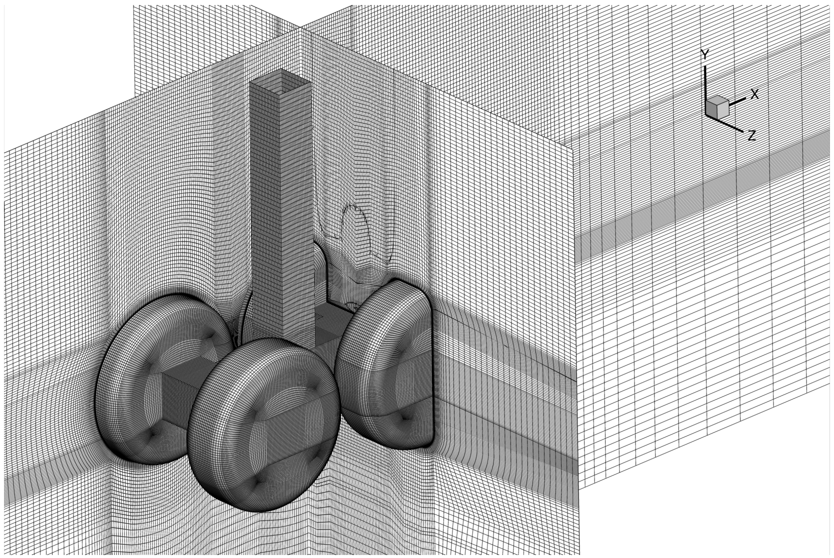

- Courtesy of L. Wang
- 37M cells
- Designed to support wave resolution up to $St \approx 10$ for 2nd order accurate solver

Unstructured grid

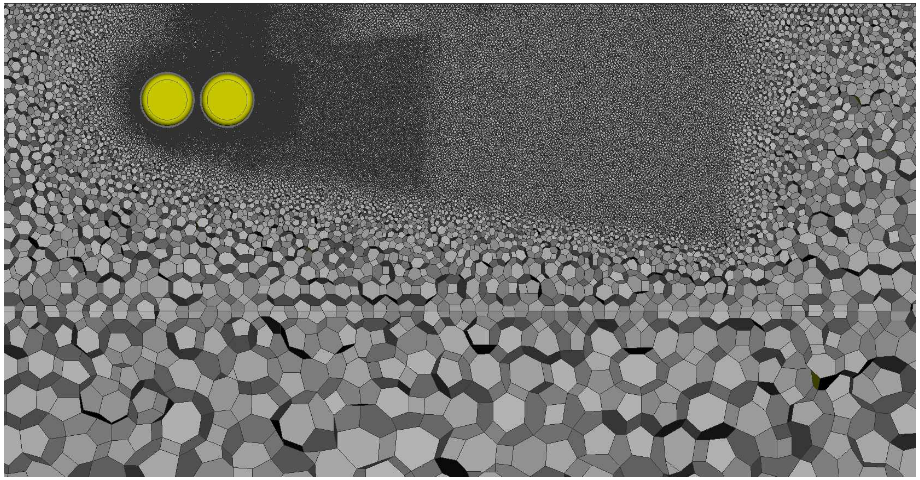

- Polyhedral mesh generated with ANSA
- 18.4M cells
- 32 prism layers, $y^+_{max} = 1.45$
- Refinement tailored to flow features

Structured and unstructured grids

Structured grid

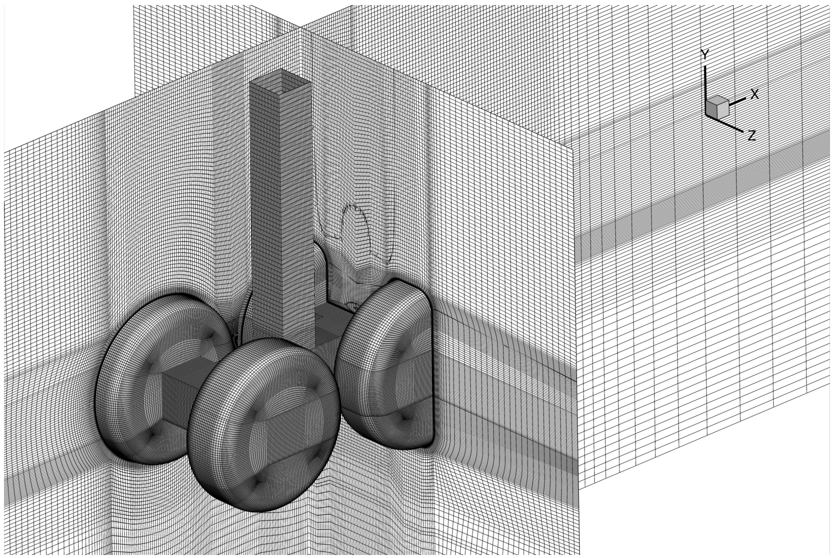

- Courtesy of L. Wang
- 37M cells
- Designed to support wave resolution up to $St \approx 10$ for 2nd order accurate solver

Unstructured grid

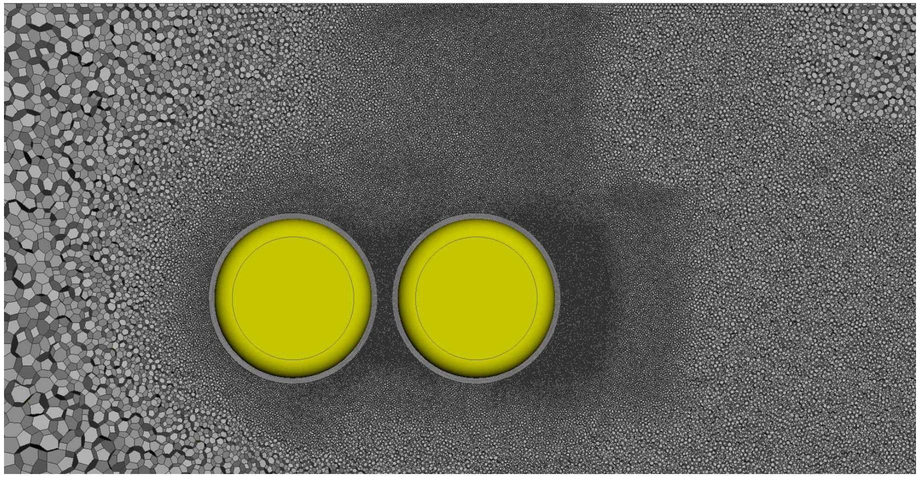

- Polyhedral mesh generated with ANSA
- 18.4M cells
- 32 prism layers, $y^{+}_{max} = 1.45$
- Refinement tailored to flow features

Structured and unstructured grids

Structured grid

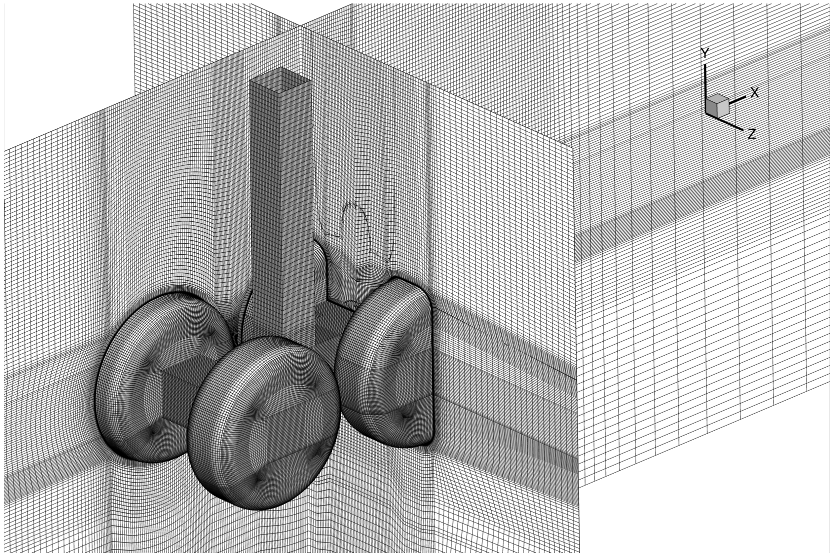

- Courtesy of L. Wang
- 37M cells
- Designed to support wave resolution up to $St \approx 10$ for 2^{nd} order accurate solver

Unstructured grid

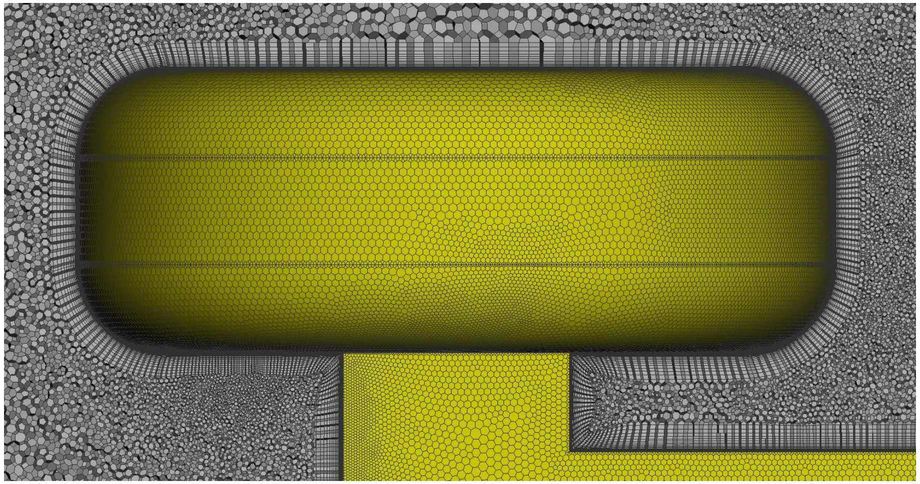

- Polyhedral mesh generated with ANSA
- 18.4M cells
- 32 prism layers, $y^+_{max} = 1.45$
- Refinement tailored to flow features

Structured and unstructured grids

Structured grid

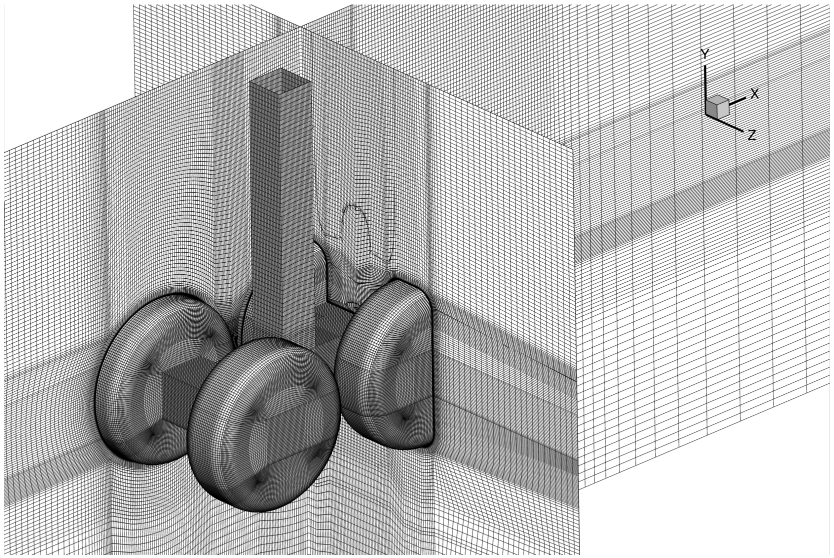

- Courtesy of L. Wang
- 37M cells
- Designed to support wave resolution up to $St \approx 10$ for 2nd order accurate solver

Unstructured grid

- Polyhedral mesh generated with ANSA
- 18.4M cells
- 32 prism layers, $y^+_{max} = 1.45$
- Refinement tailored to flow features

Aeroacoustics post-processing

- Two different strategies for surface data collection are analysed:

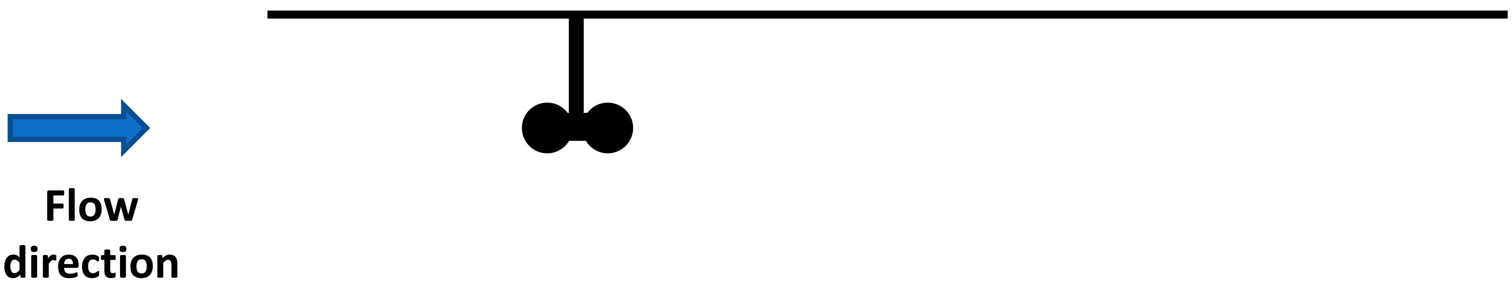

Aeroacoustics post-processing

- Two different strategies for surface data collection are analysed:

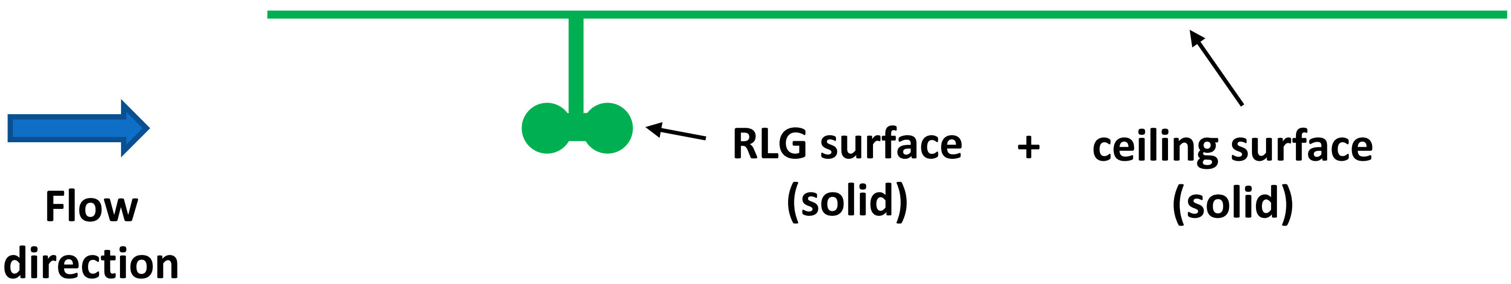

- **Curle**: only contributions of solid surfaces are considered
  - Quadrupole terms neglected
  - Including the ceiling in the analysis is indispensable to capture wave reflections

Aeroacoustics post-processing

- Two different strategies for surface data collection are analysed:

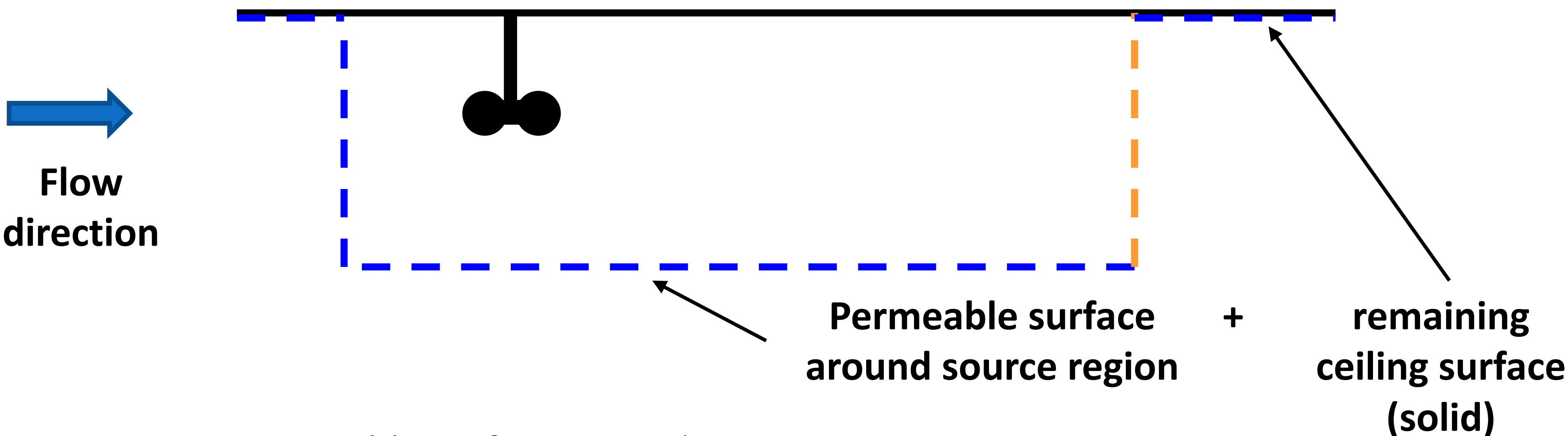

- **FW-H**: permeable surface around acoustic source region
  - Includes all acoustic source terms
  - Treatment of closing surface downstream can have a significant influence on low-frequency noise contribution

Aeroacoustics post-processing

- Two different strategies for surface data collection are analysed:

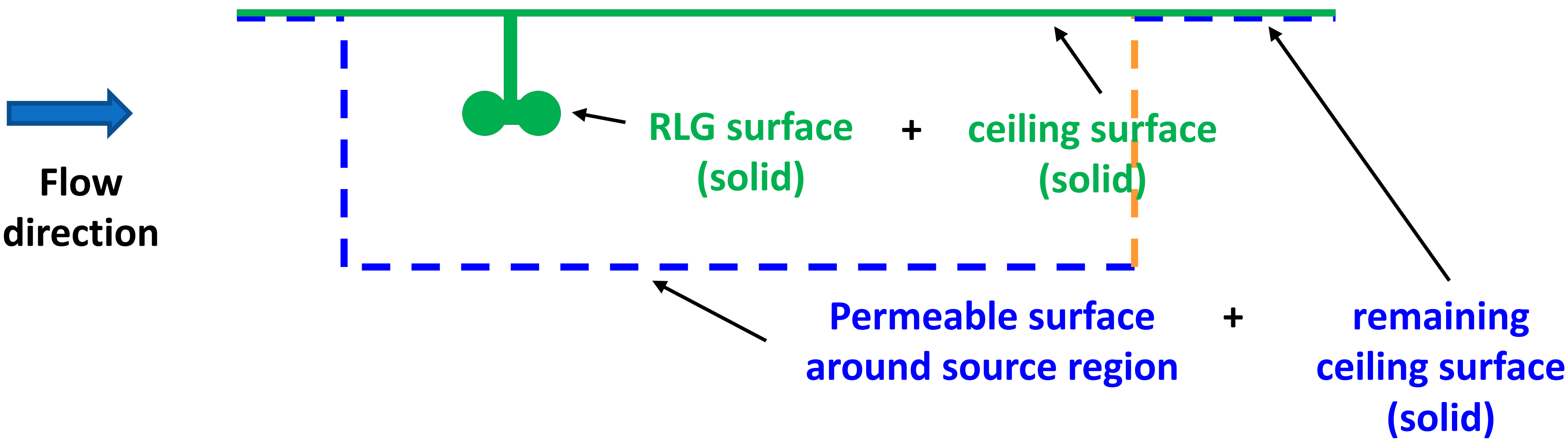

- For low Mach number flows ($M = 0.12$ in this case), both **Curle** and **FW-H** approaches are expected to deliver a comparable prediction for the far-field sound, as the role of quadrupoles should be minor

Solver comparison (structured grid)

Standard solver

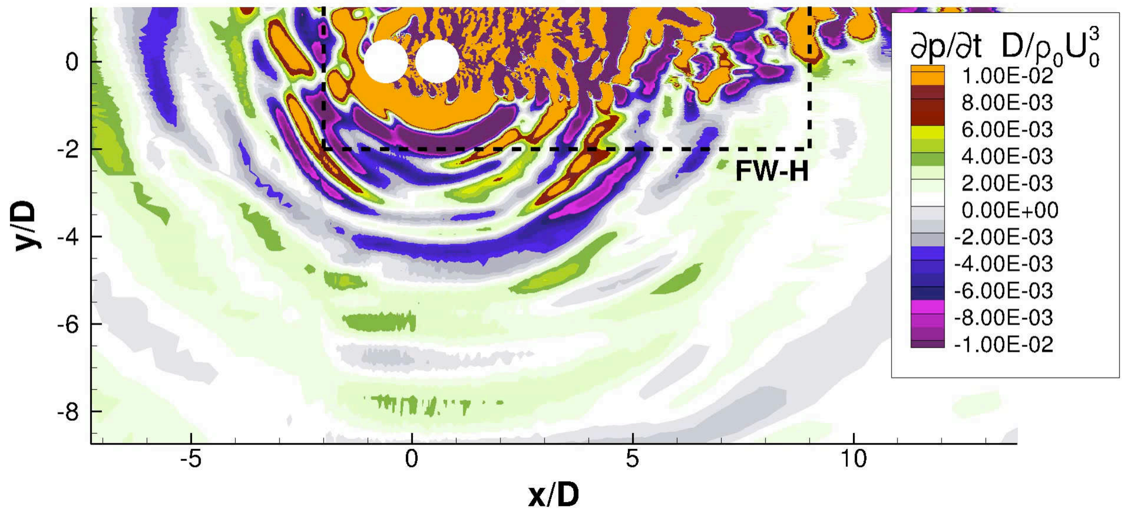

Improved solver

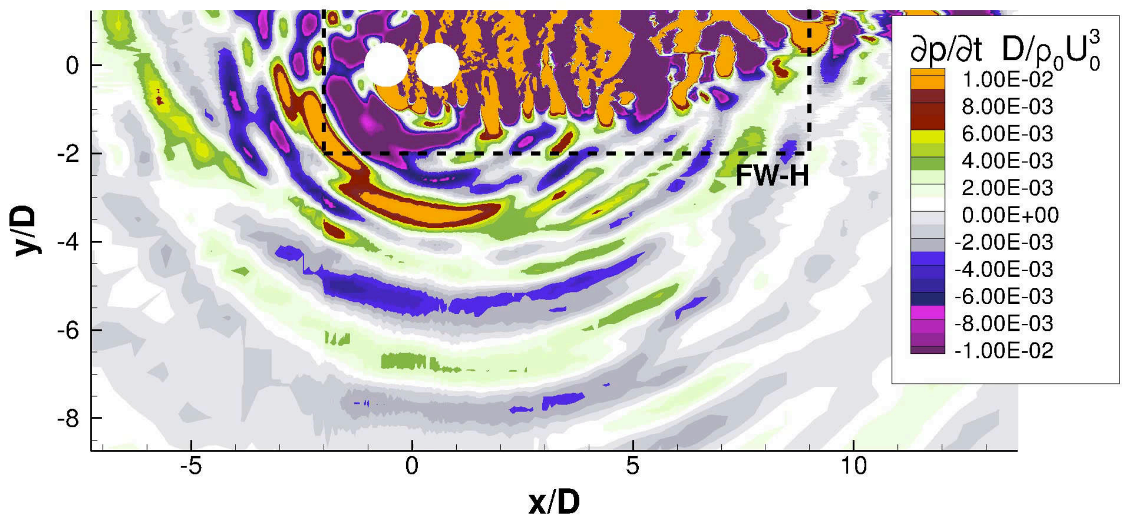

Solver comparison (structured grid)

Standard solver

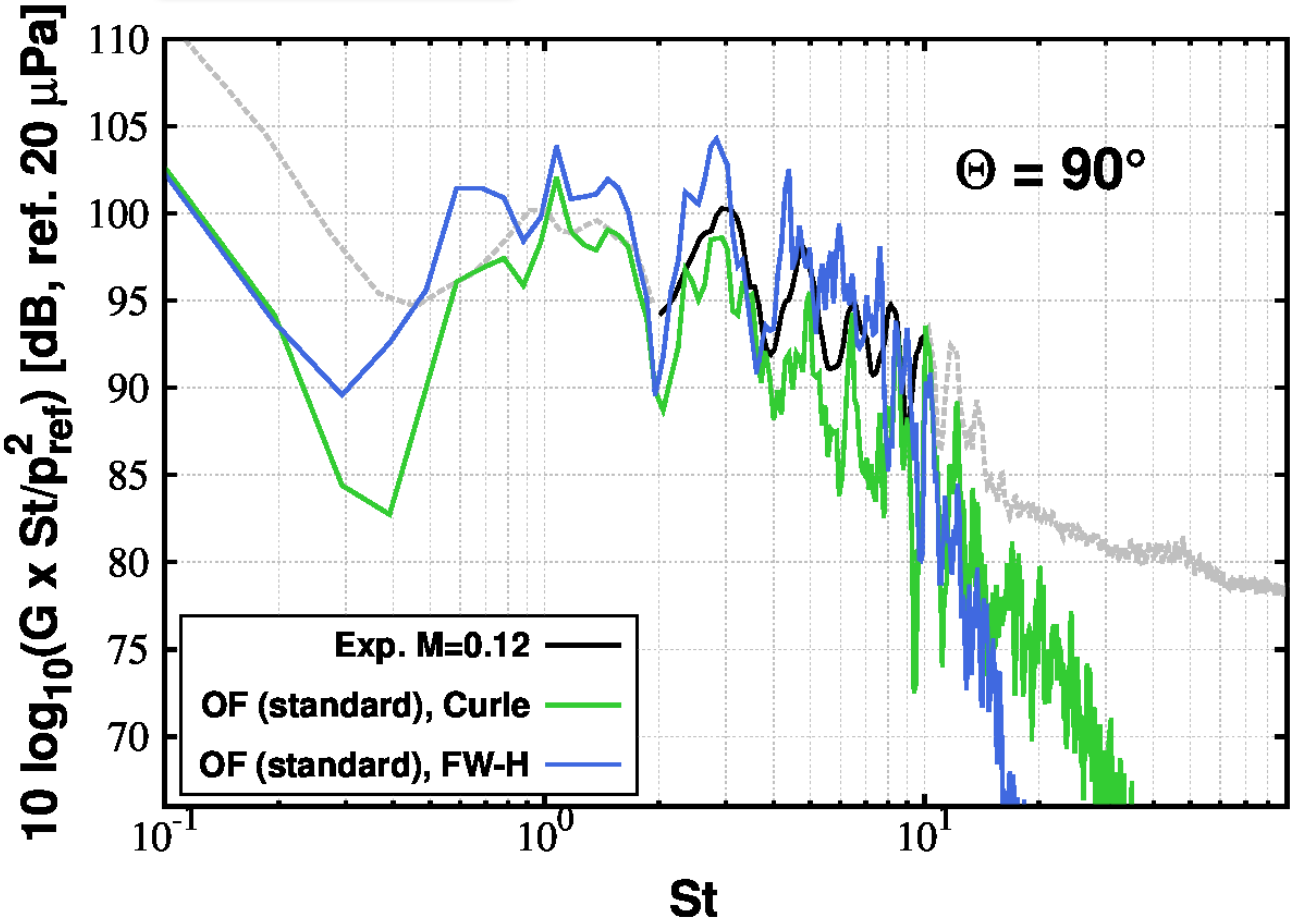

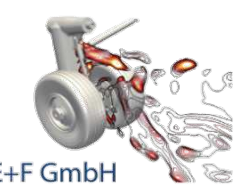

Solver comparison (structured grid)

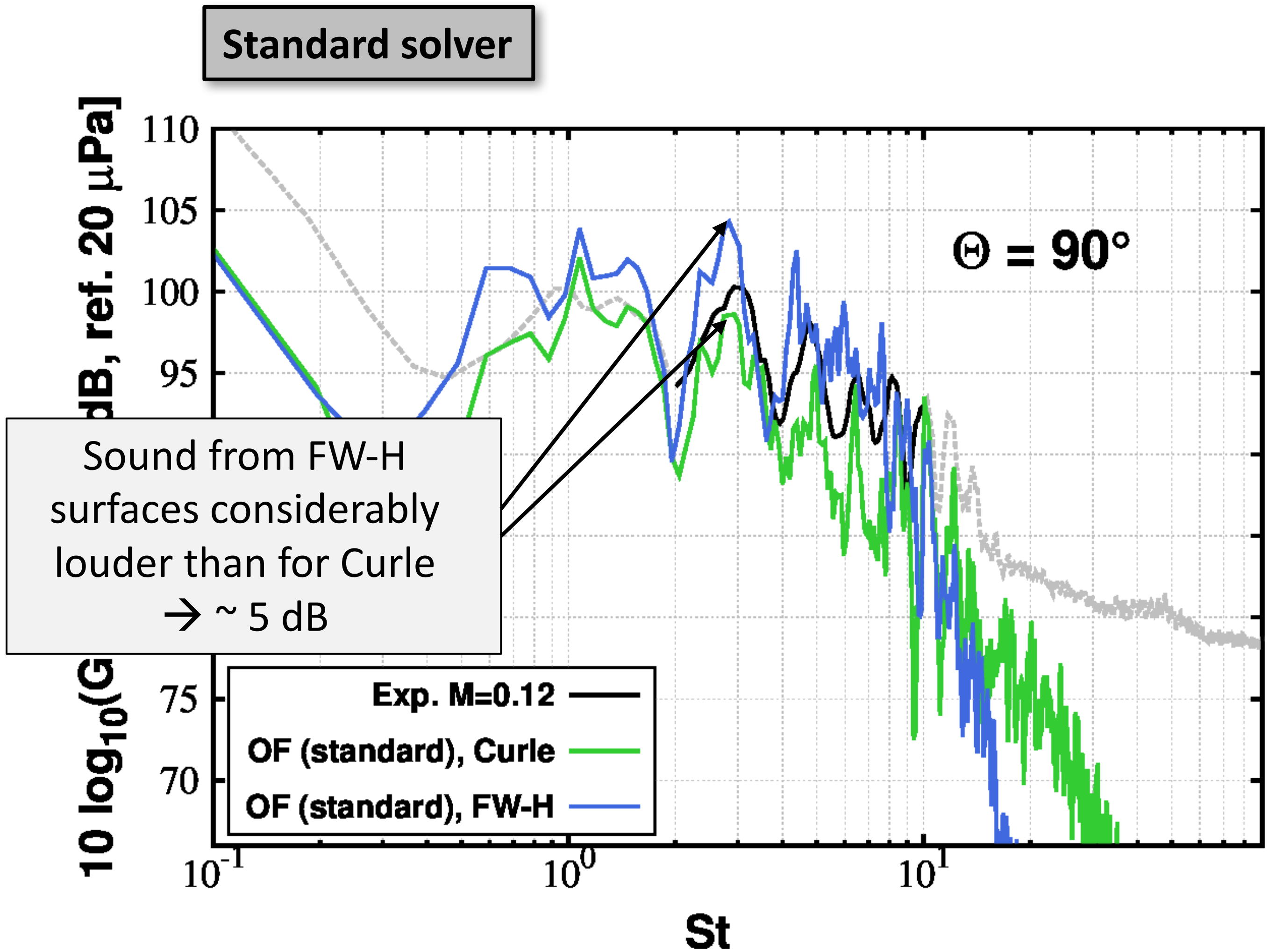

Solver comparison (structured grid)

Standard solver

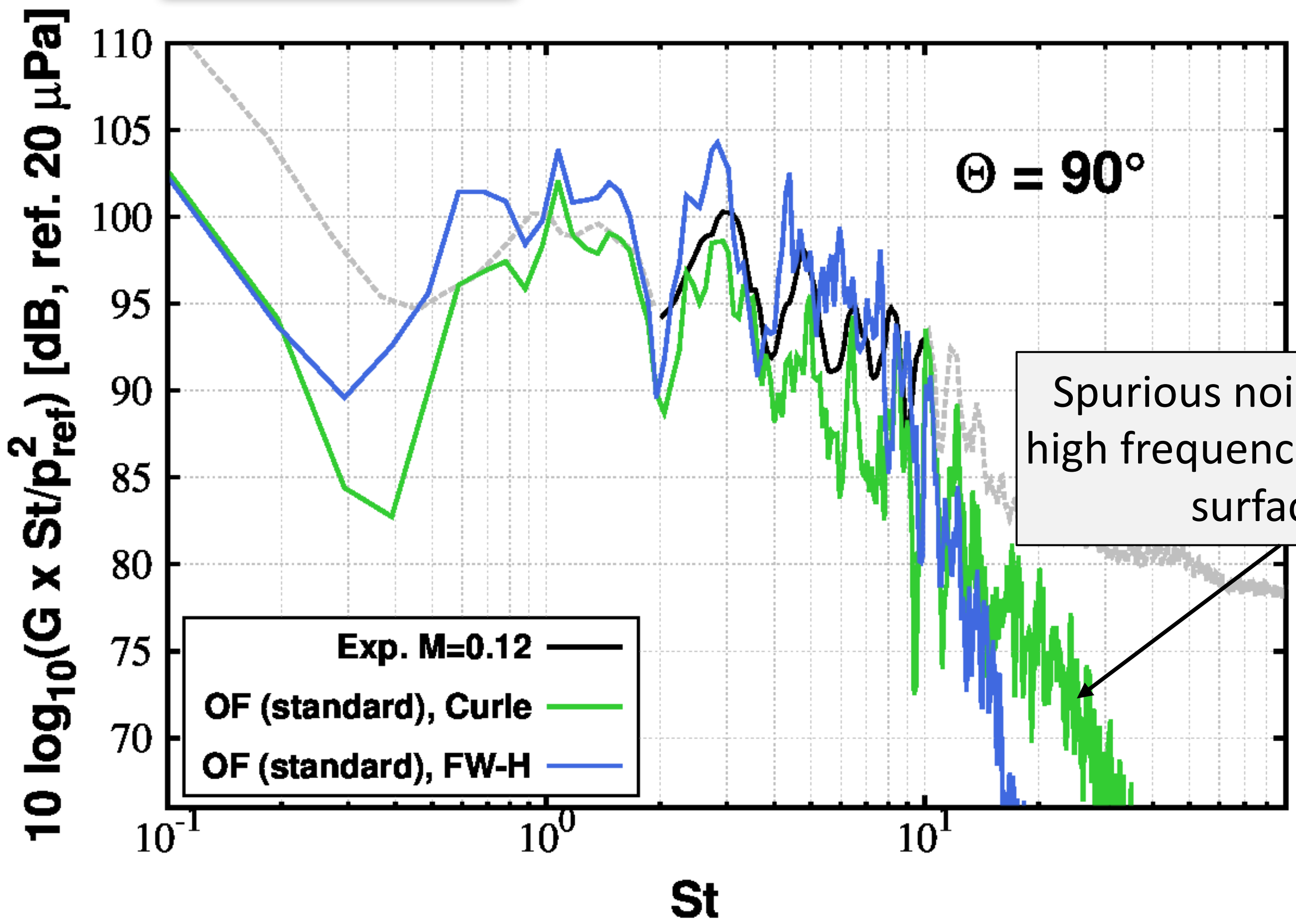

Spurious noise seen at high frequencies for solid surfaces

Solver comparison (structured grid)

Improved solver

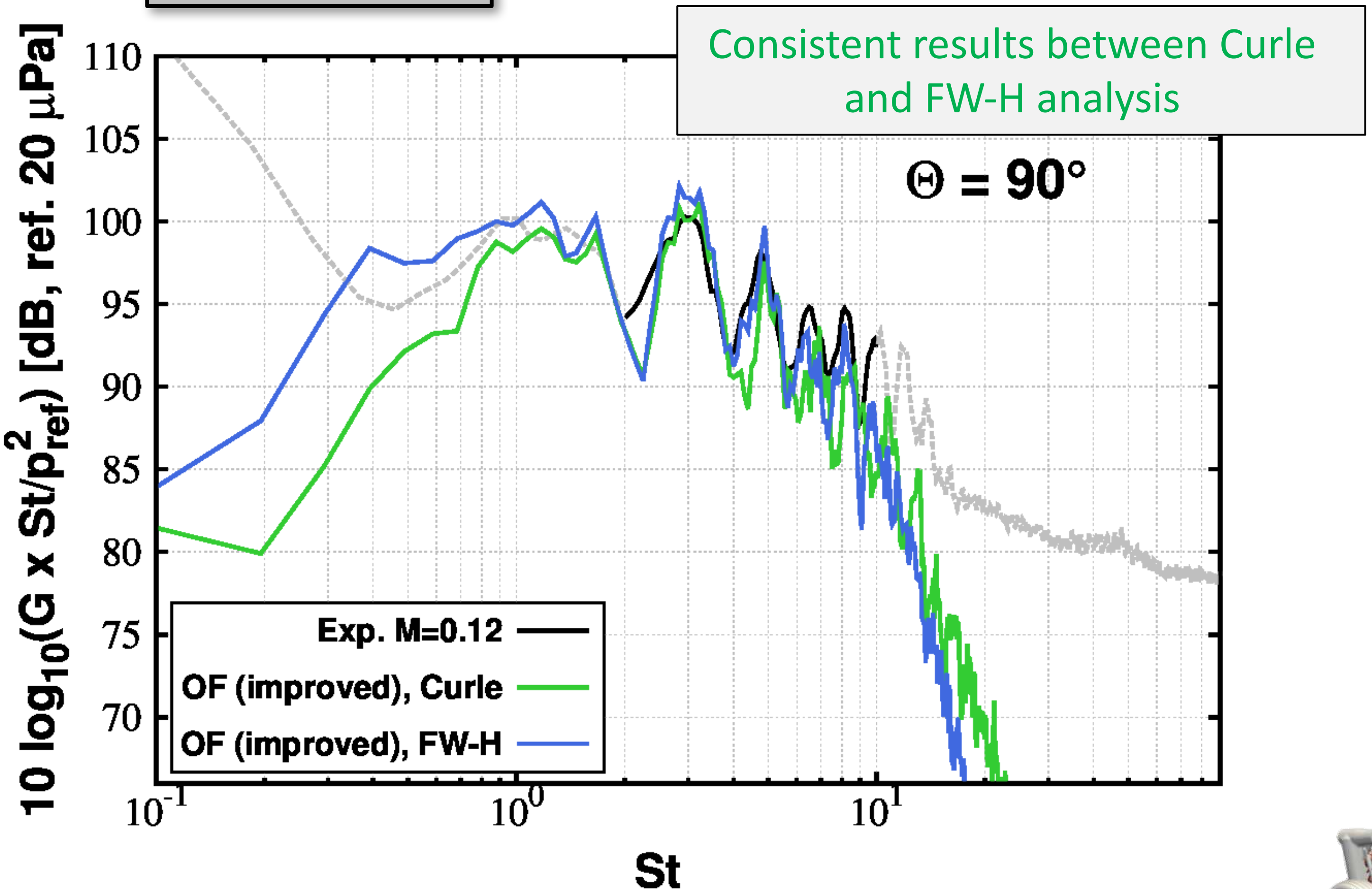

Grid comparison (improved solver)

Snapshots of flow and acoustic fields

Unstructured grid

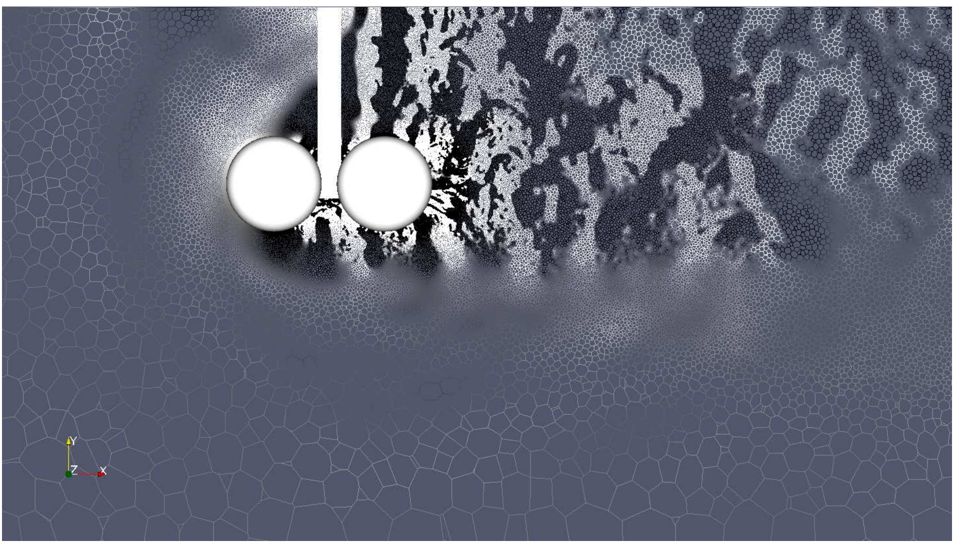

Structured grid

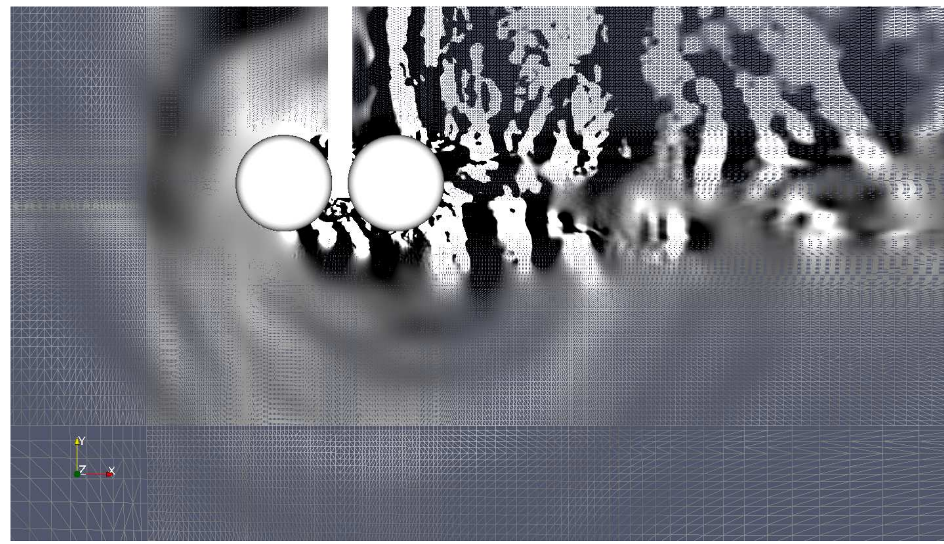

Grid comparison (improved solver)

Snapshots of flow and acoustic fields

Unstructured grid

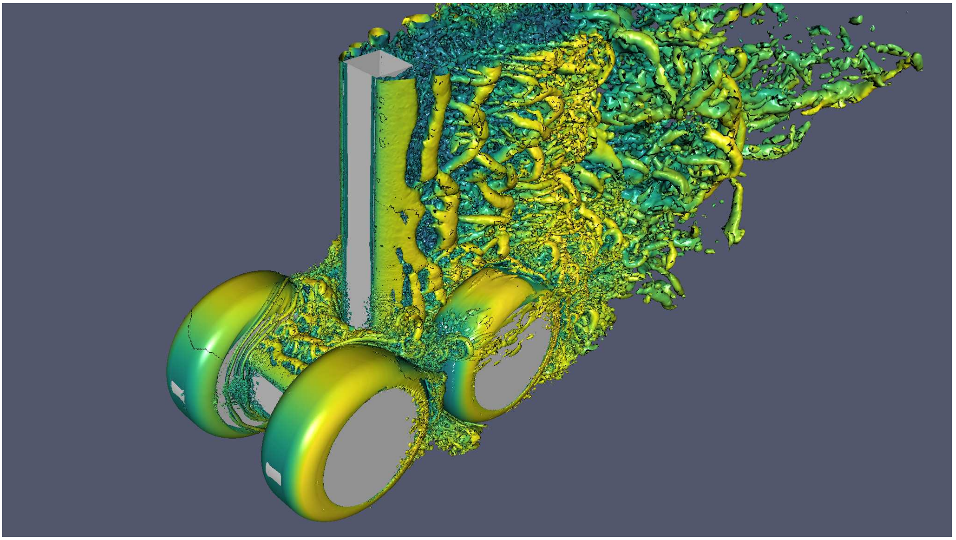

Structured grid

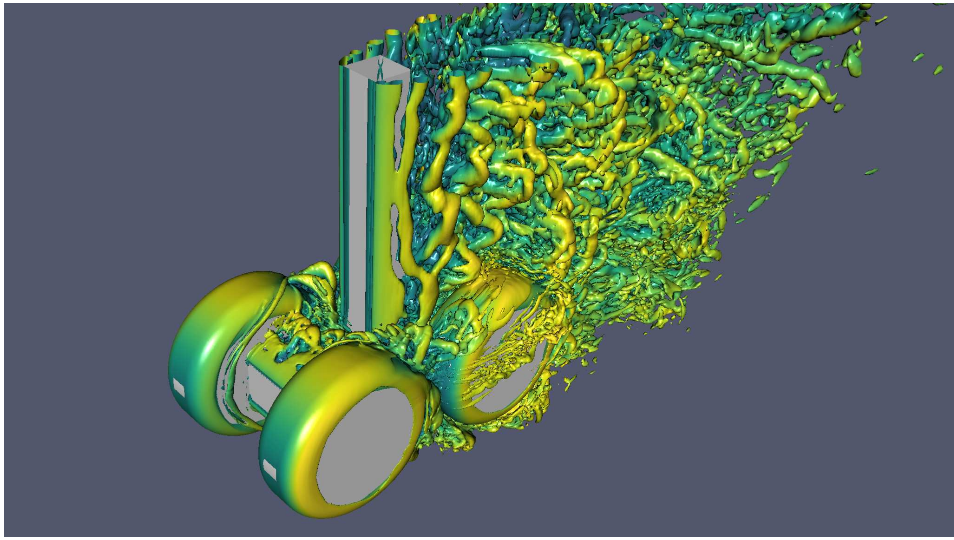

Finer turbulence resolution on unstructured grid
…but also some spurious structures?

Grid comparison (improved solver)

Snapshots of flow and acoustic fields

Unstructured grid

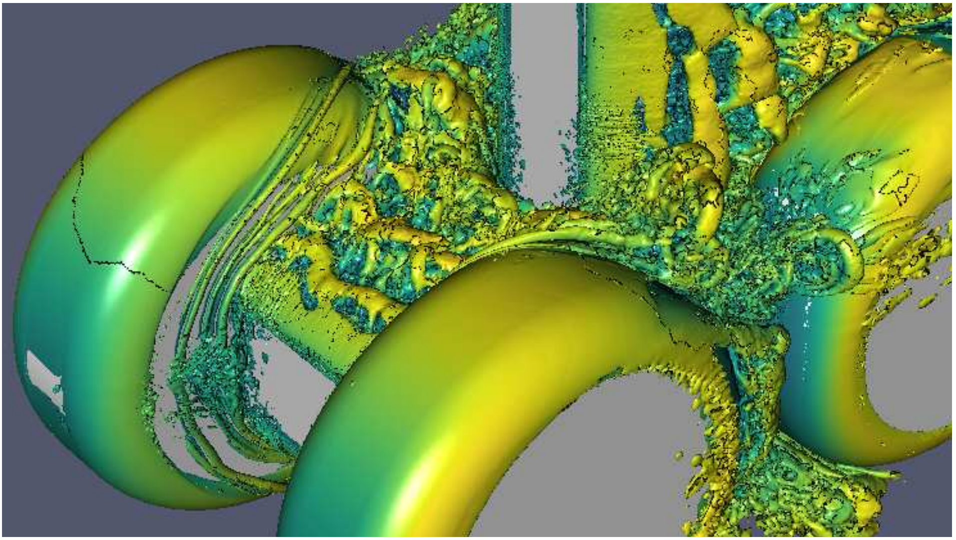

Structured grid

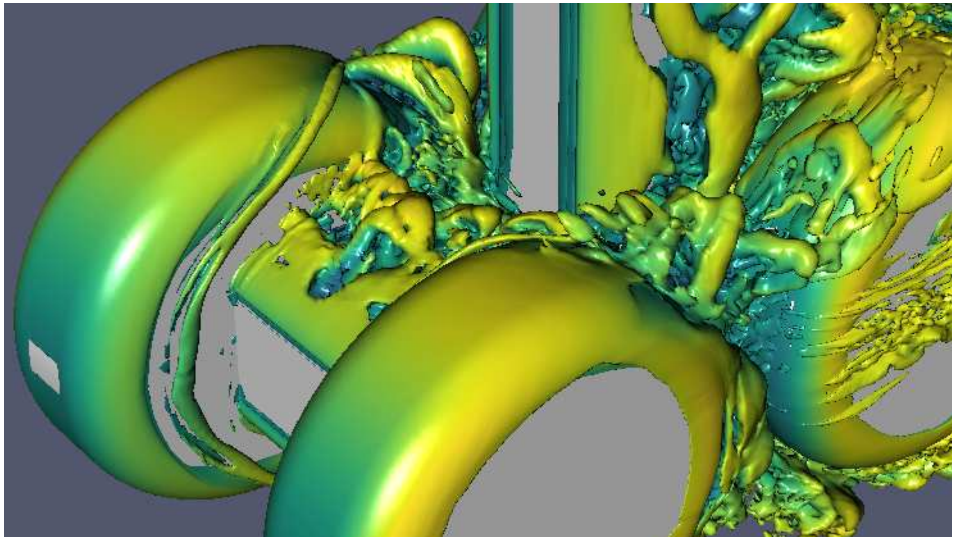

Finer turbulence resolution on unstructured grid
…but also some spurious structures?

Grid comparison (improved solver)

Snapshots of flow and acoustic fields

Unstructured grid

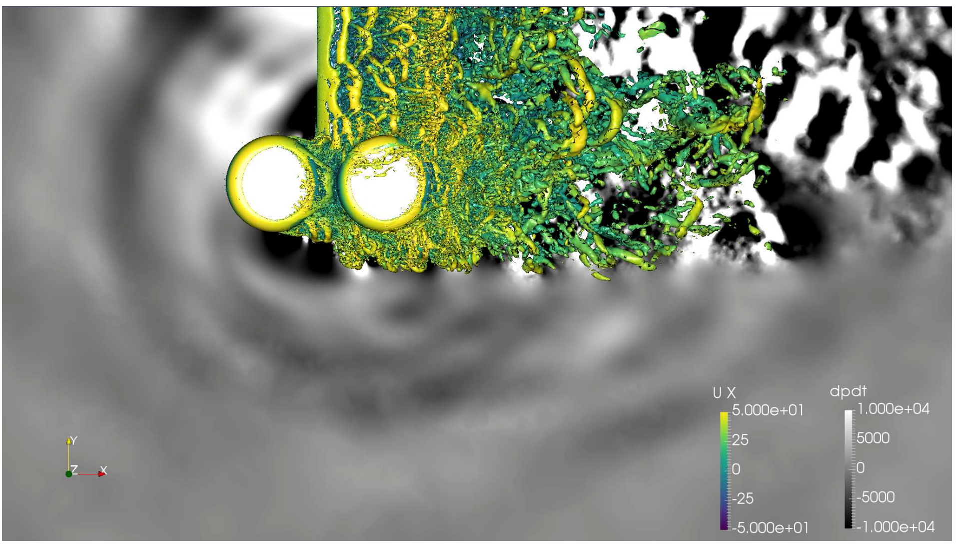

Structured grid

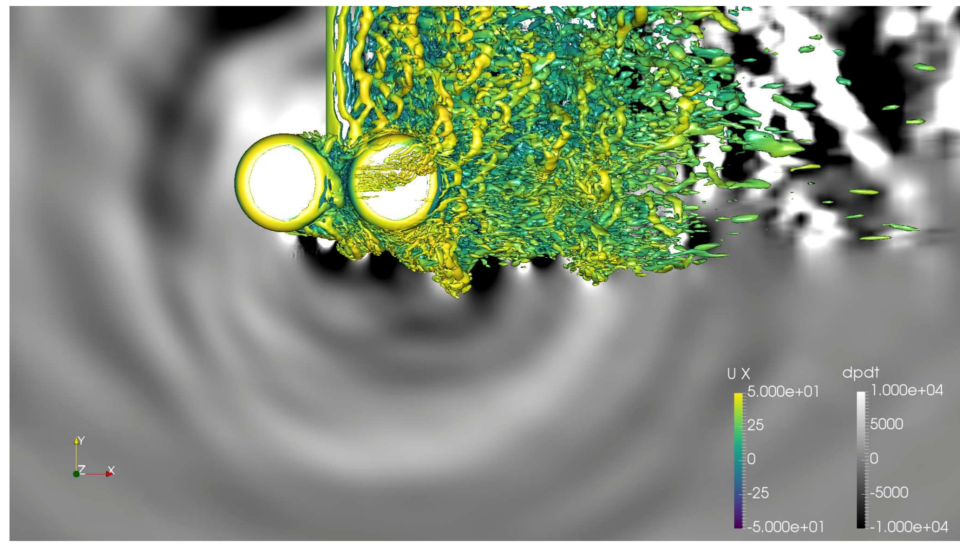

Finer turbulence resolution on unstructured grid
…but also some spurious structures?

Grid comparison (improved solver)

Snapshots of flow and acoustic fields

Unstructured grid

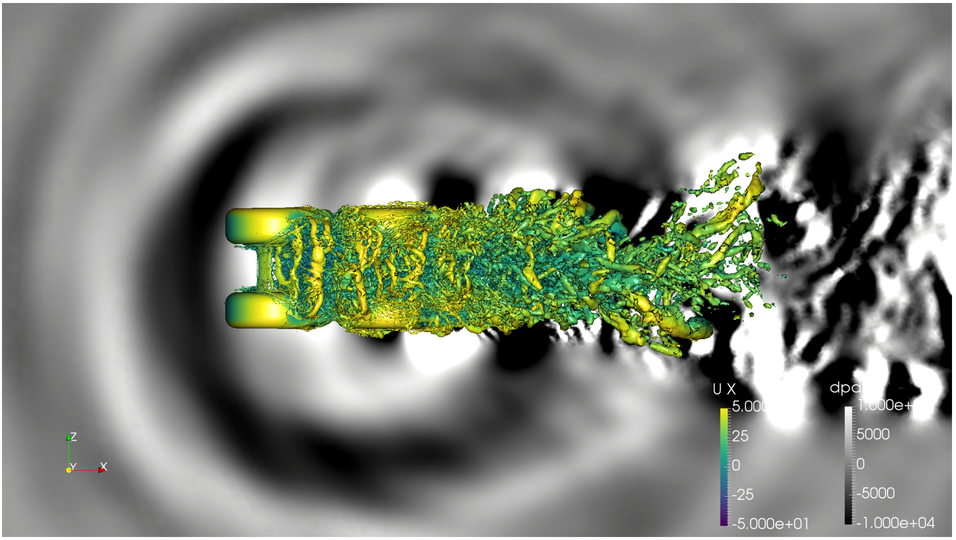

Structured grid

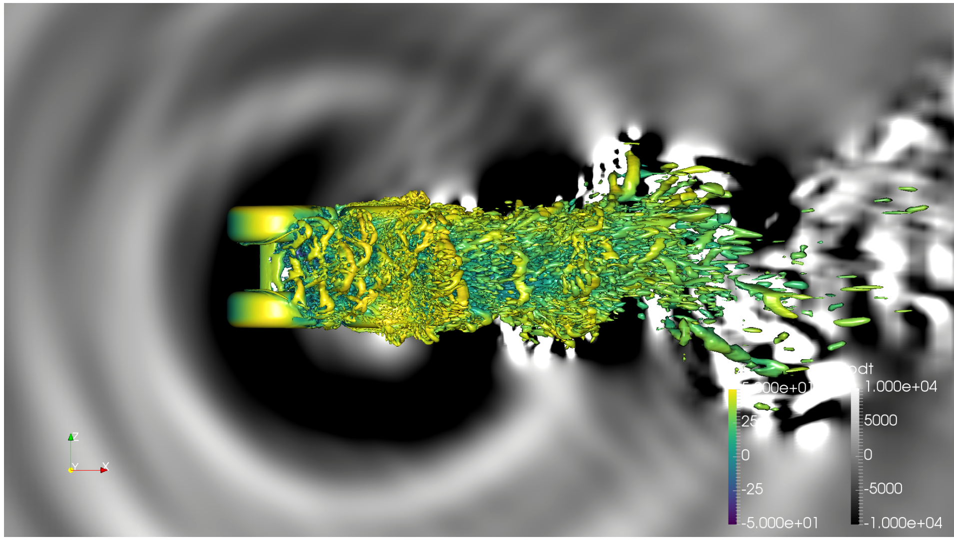

Finer turbulence resolution on unstructured grid
…but also some spurious structures?

Far-field sound spectra

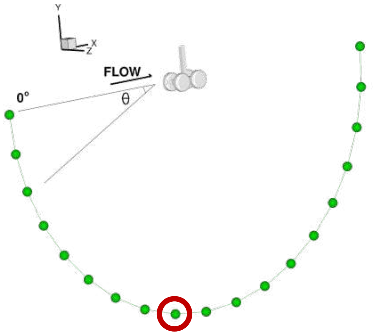

Structured (green) and unstructured (blue) meshes
All with improved solver
Comparison of permeable and solid integration surfaces

Permeable (FW-H)

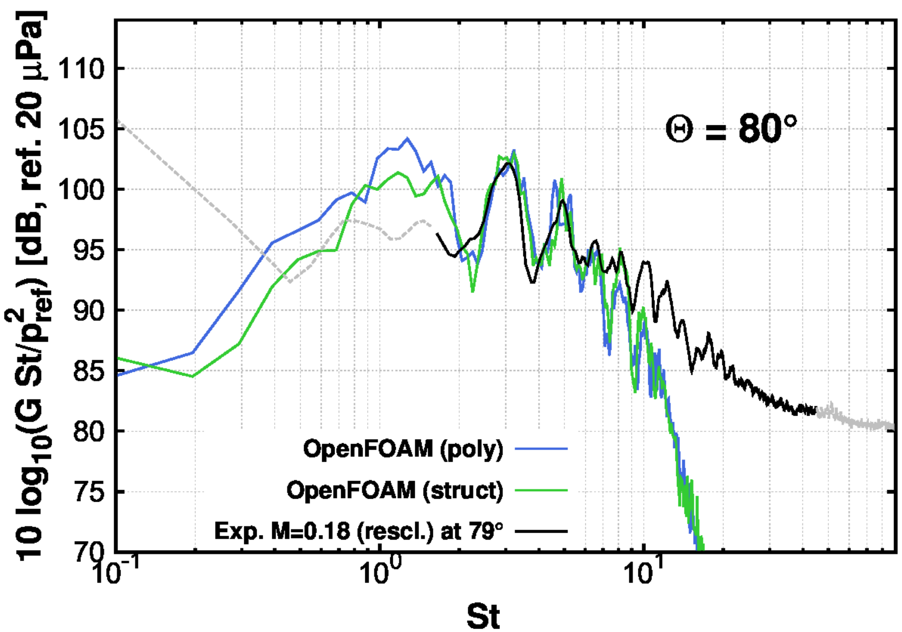

Solid (Curle)

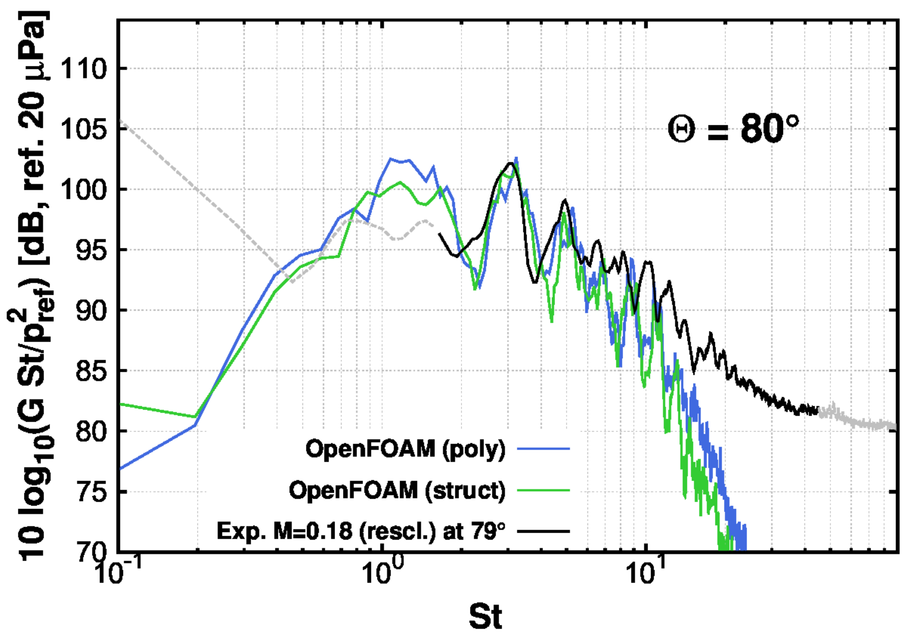

Far-field sound spectra

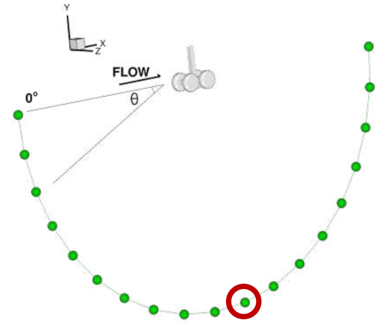

Structured (green) and unstructured (blue) meshes

All with improved solver

Comparison of permeable and solid integration surfaces

Permeable (FW-H)

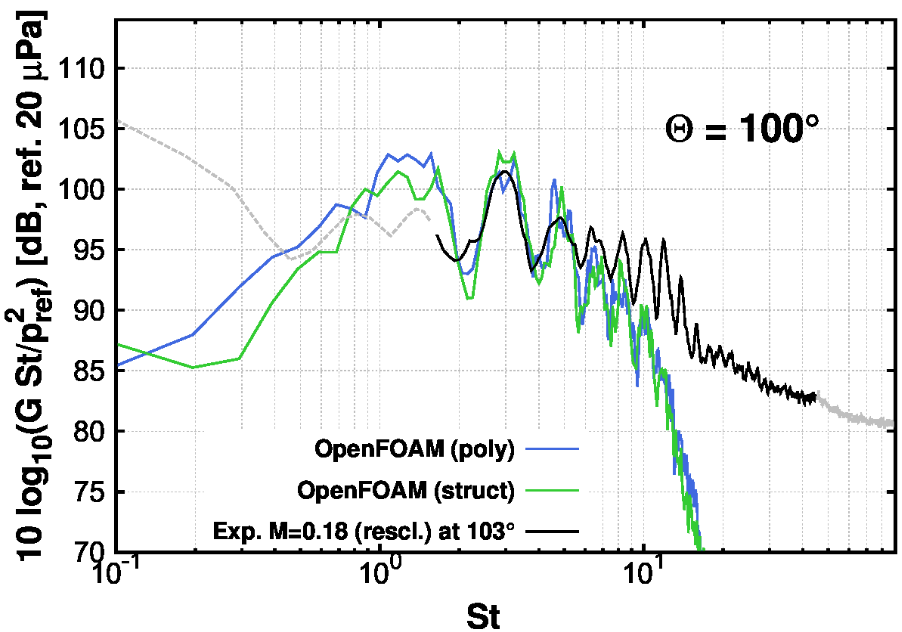

Solid (Curle)

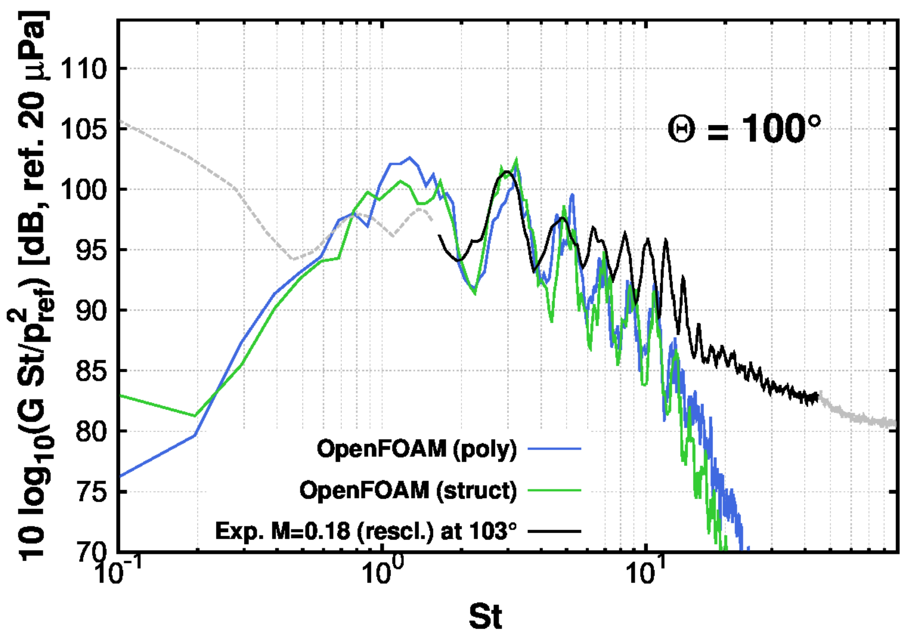

Far-field sound spectra

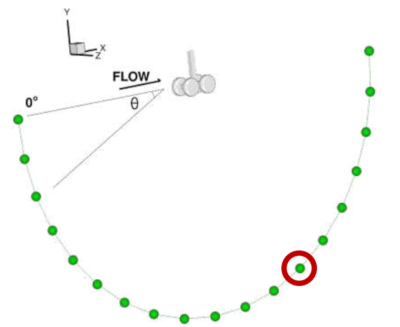

Structured (green) and unstructured (blue) meshes
All with improved solver
Comparison of permeable and solid integration surfaces

Permeable (FW-H)

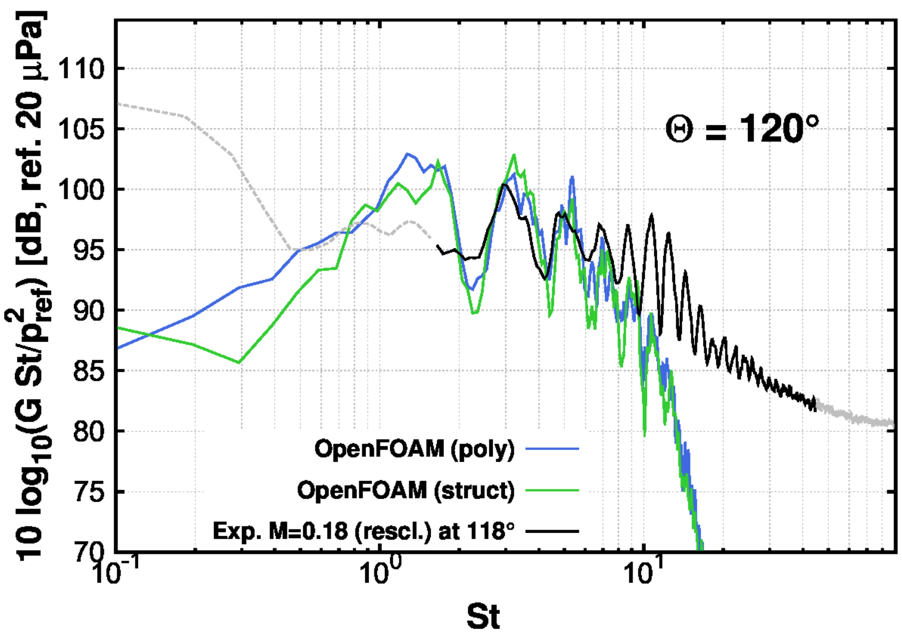

Solid (Curle)

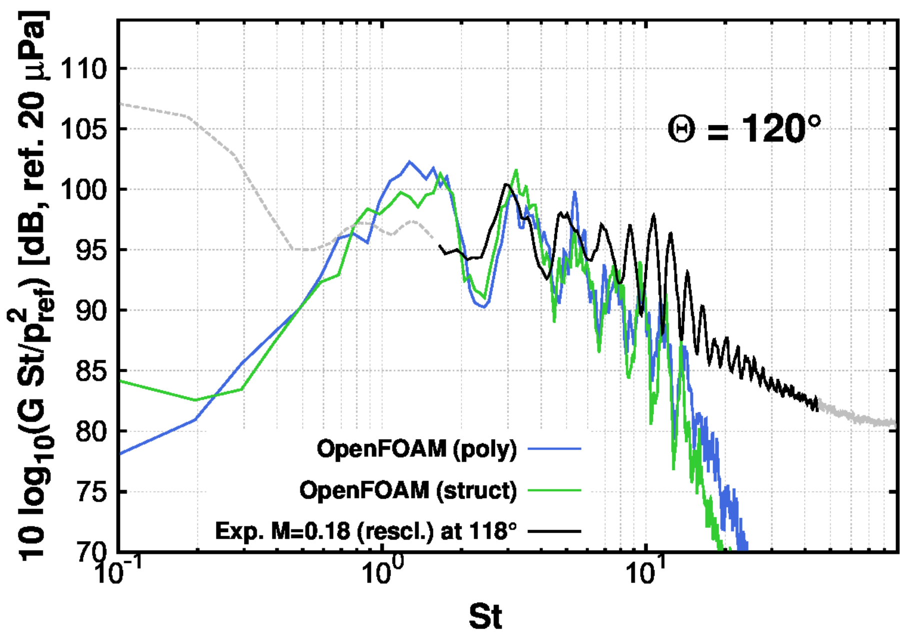

Comparison with BANC-II results

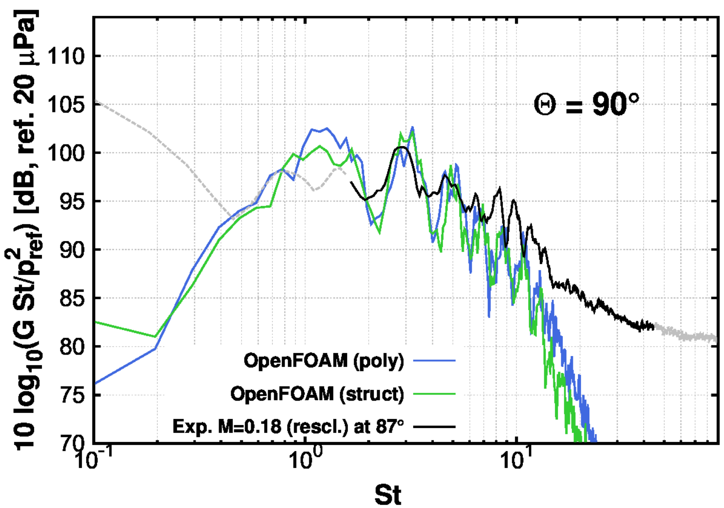

Improved solver, both meshes

Blind partner results from BANC-II workshop

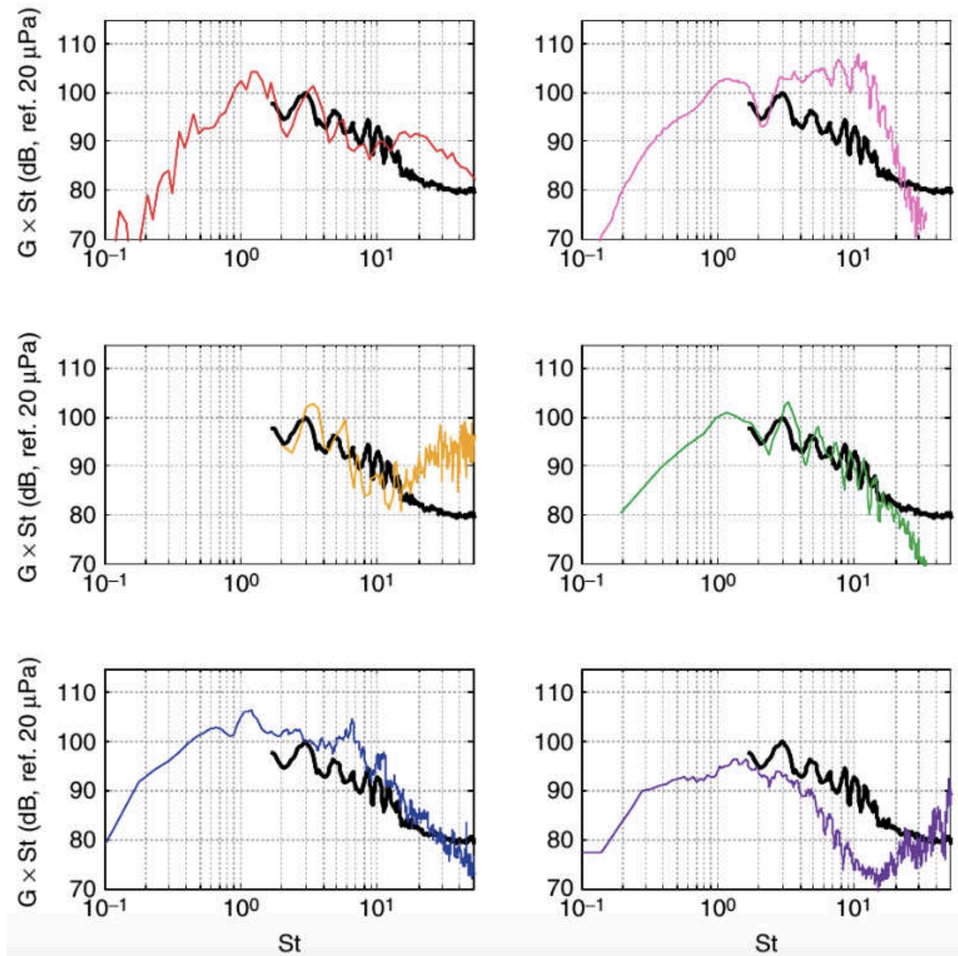

- Very competitive level of agreement
- No spurious noise despite unstructured grid
- Slightly less high-frequency resolution than previous results with in-house code (green data on right)

Introduction

Enhanced aeroacoustics features in OpenFOAM

- Improved aeroacoustics solver for low Mach number applications
- Efficient input / output library for FW-H analysis
- Improved hybrid RANS-LES turbulence modelling

Validation for Rudimentary Landing Gear

- Test case setup
- Solver comparison
- Mesh comparison

Conclusions and next steps

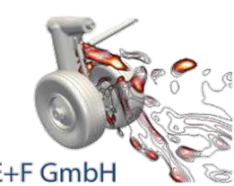

Conclusions

- Complete process chain for aeroacoustic simulation validated with satisfactory results for a very challenging test case
- Standard OpenFOAM solver returns unreliable aeroacoustic prediction:
  - Physically inconsistent behaviour seen between Curle and FW-H post-processing
- Improved pressure-based acoustics solver shows a very consistent performance for the RLG:
  - Very competitive performance relative to other CFD solvers
  - Faster convergence and therefore 33% lower CPU time relative to standard solver
- First validation also on unstructured meshes:
  - Unstructured mesh resolves finer structures than structured mesh
  - Far-field spectra for unstructured mesh agree slightly better with measurements
  - No spurious acoustic content detected on unstructured mesh
- OpenFOAM results resolve spectra up to $St \approx 6$ whereas in-house code resolves up to $St \approx 10$ (same grid and time step)
  - “Cancellation of errors” in previous results?
  - Finer mesh and/or time step?

Thank you for your attention